



ChemComm

In situ formic acid dehydrogenation observation using UV-Vis-diffuse-reflectance spectroscopy system

Journal:	<i>ChemComm</i>
Manuscript ID	CC-COM-07-2022-003768.R1
Article Type:	Communication

SCHOLARONE™
Manuscripts

COMMUNICATION

In situ formic acid dehydrogenation observation using UV-Vis-diffuse-reflectance spectroscopy system

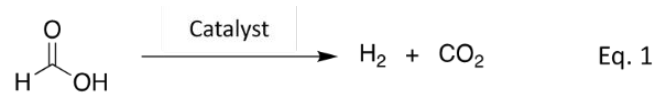
Received 00th January 20xx,

Accepted 00th January 20xx

DOI: 10.1039/x0xx00000x

By applying a simple method on the generated gas concentration in the center of a round cell through high-speed stirring, we succeeded in continuously monitoring the catalytic formic acid dehydrogenation using a newly developed in-situ/operand UV-Vis-diffuse-reflectance spectroscopy system which can exhibit a high S/N ratio and reliable spectra without any mechanical errors from gas meters.

In recent years, hydrogen has garnered considerable attention as a potential green energy source for a sustainable society. Several approaches, such as fuel cells (FCs) for mobility in various sectors, are currently under investigation to explore how to use hydrogen to meet the growing energy demand of human activities. One of the challenges to the widespread application of hydrogen energy is its low economic benefits. In recent decades, formic acid (FA), which possesses a high hydrogen content (53 g of H₂/L) and is nontoxic, has garnered considerable attention. FA is regarded as one of the most promising liquid hydrogen carriers.¹⁻³ The catalytic formic acid dehydrogenation (FADH) generates hydrogen along with CO₂, as expressed in equation 1.



With regard to formic acid dehydrogenation (FADH), researchers have mainly focused on the development of efficient catalysts; thus, a myriad of homogeneous catalysts have been developed thus far (for instance, Ru⁴⁻⁷, Ir⁸⁻¹⁰, and Fe-based catalysts¹¹⁻¹³). However, few in situ measurements have been reported during the gas generation, including

theoretical studies¹⁴⁻¹⁷ and NMR analyses¹⁸⁻²¹, to understand the FADH reaction mechanism in the presence of homogeneous catalysts. One of the barriers to employing conventional in situ measurements of absorption spectra is the presence of gas-liquid mixed phases. This is because during the FADH, the gas-liquid boundaries block and scatter incident light, making it difficult to obtain accurate and reproducible spectra with sufficient S/N ratio. Herein, we developed a new in-situ UV-Vis-diffuse-reflectance spectroscopy technology to monitor the FADH reaction, which existed as a gas-liquid mixed-phase, and we also studied its kinetics in the presence of homogeneous catalysts.

As mentioned earlier, gas bubbles from the FADH, interrupt the optical path of the incident light and hinder spectral analysis. To overcome the negative impact of the UV-Vis boundary, we developed a simple gas-liquid separation pathway. When the aqueous solution in a cylindrical cell was stirred rapidly (1000 rpm), the distributed gas in the solution is gathered near the rotation axis (Figure S1a, and S2 in the SI). Additionally, the introduction of solid particles heavier than bubbles, for instance α -Al₂O₃, in the solution accelerates the gas-liquid-solid separation caused by the centrifugal force, and a vortex of the gathered gas is formed when the particles are distributed near the inner wall of the cylindrical cell (Figures 1a and S1b in the SI). After the separation, when the incident light from the UV-Vis spectrometer irradiated to the cell, most of the light was diffusely reflected by the particles near the inner wall of the cell (Figure 1b). Thereafter, the reflected light was collected by concave mirrors and finally recorded by the detector of the spectrometer (Figures S3, S4, and S5 in the SI). To analyse the resultant spectra, the obtained diffuse reflectance spectra were converted into absorption spectra using the Kubelka-Munk equation (Eq. 2), where R_{∞} , K and S' represent the diffuse reflectance, absorption coefficient of the species, and scattering coefficient, respectively.

Generally, when light with a specific wavelength passes through the solution between the particles, it can be absorbed by the solute molecules. Based on this, we can detect the

$$\frac{(1 - R_{\infty})^2}{2R_{\infty}} = \frac{K}{S'} \quad \text{Eq. 2}$$

Graduate School of Pure and Applied Science, University of Tsukuba, Tsukuba, 305-8577, Japan.

National Institute of Advanced Industrial Science and Technology (AIST), Tsukuba, 305-8565, Japan.

† Footnotes relating to the title and/or authors should appear here.

Electronic Supplementary Information (ESI) available: [details of any supplementary information available should be included here]. See DOI: 10.1039/x0xx00000x

spectroscopic changes that occur during the FADH reaction in the presence of FA, catalyst, and intermediates. Thus, it enables the optical collection of in situ information from the reaction solution by detecting this diffuse reflection.

To make our method practical, we set up a UV-Vis-diffuse-reflectance spectroscopic system (Figures S3 and S5). A Cary 5000 spectrometer (Agilent Technology Inc.) was used in this system. α -Al₂O₃ (Figures S6 and S7) was used as the light-diffusing particle in our experiments. Moreover, optical absorption was observed at a wavelength range of 200–800 nm on γ -Al₂O₃, rutile-TiO₂, amorphous SiO₂, and monoclinic ZrO₂ compared with α -Al₂O₃ (Figure S8).²² To evaluate the reliability of the proposed method, we measured botanical dye (alizarin) using the proposed system and compared the results with those from a conventional UV-Vis spectrometer in a transmission mode (Figure S9a).²³ We observed that the shapes and peak positions of the spectra obtained using the proposed and conventional methods are in good agreement (Figure S10a). The proportional relationship between the K/S values at 261, 330, and 520 nm and alizarin concentrations varied from 1.04 x 10⁻⁵ mol/L to 1.89x10⁻⁴ mol/L as shown in Figure S10b.

To apply the proposed method to *in situ* investigations of FADH, we first studied the reaction at 80 °C using 98% FA in the presence of the iridium complex ([Cp*Ir(4DHBP)(OH₂)]SO₄) as a catalyst and α -Al₂O₃ (Figure 2). In comparison to the results of the conventional transmission UV-Vis spectroscopy, a reproducible spectrum with a high S/N ratio was successfully obtained using the proposed method. Notably, we also observed detectable absorption peaks of the catalyst, [Cp*Ir(4DHBP)(OH₂)]SO₄, (Figure 2b), which could not be observed using a conventional transmission UV-Vis spectrum (Figure S11). We also confirmed that FA hardly remained on the surface of α -Al₂O₃ after exhaustion of FA by its dehydrogenation, because the photo-absorption band (216 nm) of FA was not detected in the residual solution in the UV-vis absorption spectrum (Figure S12) and α -Al₂O₃ did not degrade the performance of the catalyst (Figure S13).

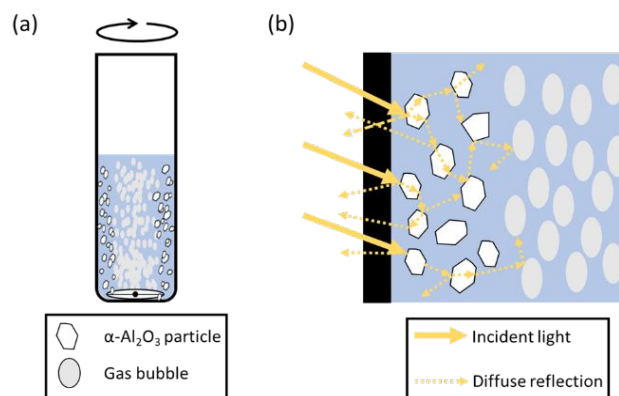


Fig.1 (a) Schematic of the distribution of gas bubbles and α -Al₂O₃ particles; and (b) the optical pathway in the sample.

For the results of the UV-Vis-diffuse-reflectance spectroscopy, we converted the diffuse reflectance spectra (Figure S14a) into absorption spectra (Figure S14b) using equation 2 to quantify the concentration of FA (peak wavelength at 215 nm) as a function of reaction time during the FADH (Figure 3). The results demonstrate that FA was completely exhausted in 4 h along with the generation of 0.69 L of gases in total during the FADH. Notably, in the initial stages of the reaction, the addition of FA caused a temperature drop in the system, which lowered the reaction rate. Moreover, the infusion error of the syringe pump results in a gap between the actual and expected volumes of FA.

In comparison with the data obtained from the spectral analysis, the gas volume detected by the gas meter was underestimated; hence, the calculated turnover frequencies (TOFs) using the spectrometer and gas meter were 5467 and 4911 h⁻¹, respectively (Figure 4). The TOFs of the former are more precise because the mechanistic measurement errors of gas meters can also lead to an underestimation of the TOF. Although the TOF in our study is almost half of the reported data (10,000 h⁻¹ at 80 °C; catalyst = [Cp*Ir(4DHBP)(H₂O)]SO₄, FA

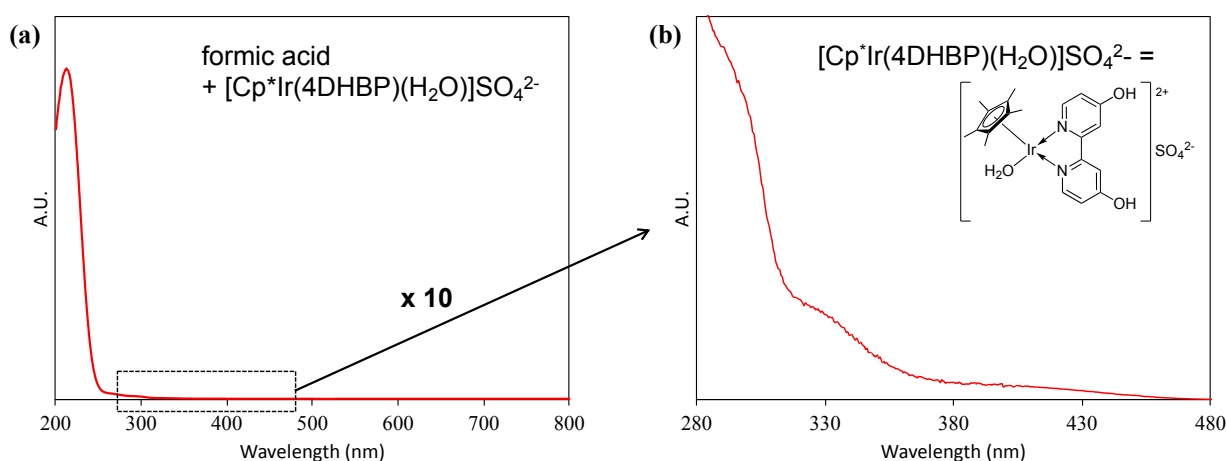


Fig.2 (a) Absorption spectrum of the sample obtained through UV-Vis-diffuse-reflectance spectroscopy; (b) The magnification of the absorption spectrum of UV-Vis-diffuse-reflectance spectroscopy (280–480nm). The sample (20mL) consisted of 0.66 M of FA, 40 μ M of [Cp*Ir(4DHBP)(OH₂)]SO₄ and 0.1 M of α -Al₂O₃.

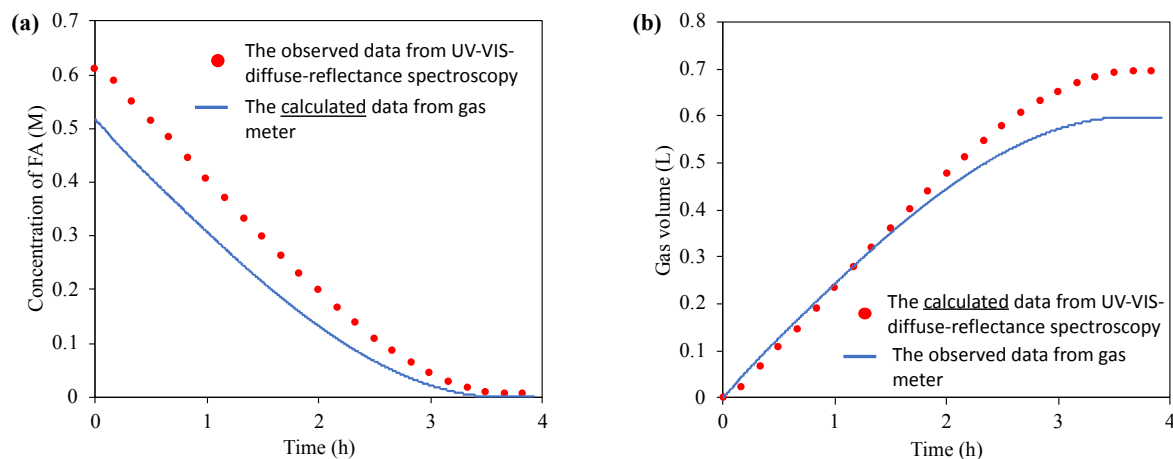


Fig.3 (a) Concentration of FA during the FADH; (b) The volume of the generated gases during the FADH. The data were calculated based on the UV-Vis-diffuse-reflectance spectra (red spot) and the gas volume measured by the gas meter (blue curve). The sample (20 mL) is consisted of 0.66 M of FA, 40 μM of $[\text{Cp}^*\text{Ir}(\text{4DHBP})(\text{OH}_2)]\text{SO}_4$ and 0.1 M of $\alpha\text{-Al}_2\text{O}_3$. Temperature: 80 $^\circ\text{C}$.

and the catalyst concentrations were 2 M and 2 μM , respectively).⁸ It is plausible that the concentration of FA and the catalyst significantly affected the initial TOFs. The turnover number (TON), which reached 15,094 at the termination of the FADH reaction, confirmed the completion of FADH using both diffuse-reflectance UV-Vis and liquid chromatography (Figure S15). From the perspective of kinetics, the activation energy ($E_a = 65.0$ kJ/mol) was calculated by the Arrhenius plot using the results obtained from the proposed method, which was 6.7 kJ/mol smaller than the previously reported value ($E_a = 71.7$ kJ/mol)¹⁷ (Figure 5).

In conclusion, we developed a new *in situ* UV-Vis-diffuse-reflectance spectroscopy system to monitor the catalytic FADH.

Using this strategy, we obtained a TOF of 5,467 h^{-1} and TON of 15,094 for the FADH reaction catalysed by $[\text{Cp}^*\text{Ir}(\text{4DHBP})(\text{H}_2\text{O})]\text{SO}_4$. The successful application of this method was confirmed by the good agreement of the obtained results with previous studies. In comparison with the data obtained from a gas meter, the proposed method can measure the data more precisely without any mechanical issues. This system can be applied to a variety of reactions in the gas-liquid heterogeneous phases even when heterogeneous catalysts are used.

This study was financially supported by the CANON foundation and the New Energy and Industrial Technology Development Organization (NEDO). The authors thank Dr. Maya

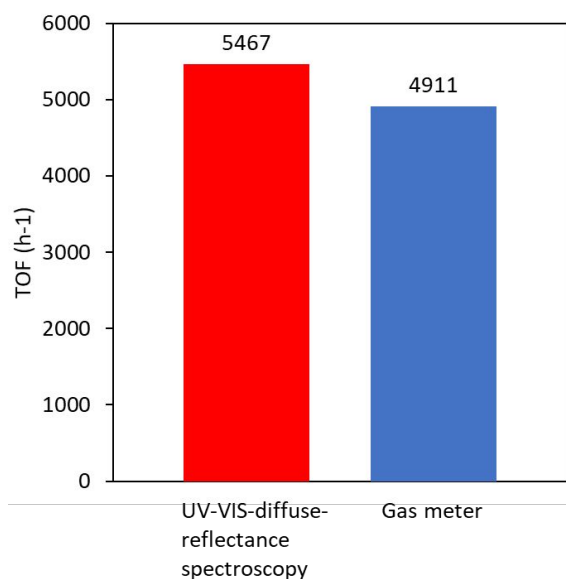


Fig. 4. TOF of the FAHD reaction at 80 $^\circ\text{C}$ calculated by using the data of UV-Vis-diffuse-reflectance spectroscopy (red) and that of the gas meter (blue), respectively.

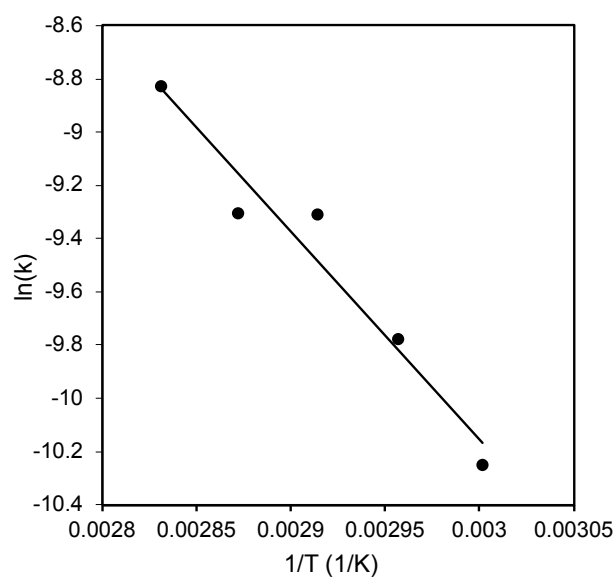


Fig. 5. Arrhenius plot of the FADH reaction catalyzed by $[\text{Cp}^*\text{Ir}(\text{4DHBP})(\text{OH}_2)]\text{SO}_4$. Reaction conditions: 60–80 $^\circ\text{C}$, FA (0.66 M, 0.5 mL), and catalyst (8×10^{-4} mmol, 0.5 mg).

Chatterjee for her checking and correcting the English language in of our manuscript. The authors declare that there are no conflicts of interests.

- 1 Kawanami, H., Himeda, Y. and Laurency, G., *Advances in inorganic chemistry*, 2017, **70**, 395-427.
- 2 Younas, M., Rezakazemi, M., Arbab, M. S., Shah, J. and Rehman, W. U., *International Journal of Hydrogen Energy*, 2022, **47**, 11694-11724.
- 3 Dutta, I., Chatterjee, S., Cheng, H., Parsapur, R. K., Liu, Z., Li, Z., Ye, E., Kawanami, H., Low, J. S. C., Lai, Z., Loh, X. J., Huang, K.-W., *Adv. Energy Materials*, 2022, **12**, 2103799.
- 4 Patra, S., Deka, H. and Singh, S. K., *Inorganic Chemistry*, 2021, **60**, 14275-14285.
- 5 Yuranov, I., Autissier, N., Sordakis, K., Dalebrook, A. F., Grasmann, M., Orava, V., Cendula, P., Gubler L. and Laurency, G., *ACS Sustainable Chem. Eng.*, 2018, **6**, 6635-6643.
- 6 Guan, C., Zhang, D. D., Pan, Y., Iguchi, M., Ajitha, M. J., Hu, J., Li, H., Yao, C., Huang, M.H., Min, S., Zheng, J., Himeda, Y., Kawanami, H. and Huang, K. W., *Inorganic Chemistry*, 2017, **56**, 438-445.
- 7 Xin, Z., Zhang, J., Sordakis, K., Beller, M., Du, C. X., Laurency, G. and Li, Y., *ChemSusChem*, 2018, **11**, 2077-2082.
- 8 Himeda, Y., *Green Chemistry*, 2009, **11**, 2018-2022.
- 9 Celaje, J. J. A., Lu, Z., Kedzie, E. A., Terrile, N. J., Lo, J. N. and Williams, T. J., *Nature communications*, 2016, **7**, 1-6.
- 10 Zhan, Y., Shen, Y., Du, Y., Yue, B. and Zhou, X., *Kinetics and Catalysis*, 2017, **58**, 499-505.
- 11 Boddien, A., Mellmann, D., Gärtner, F., Jackstell, R., Junge, H., Dyson, P. J., Beller, Laurency G., Ludwig R. and Beller M., *Science*, 2011, **333**, 1733-1736.
- 12 Curley, J. B., Bernskoetter, W. H. and Hazari, N., *ChemCatChem*, 2020, **12**, 1934-1938.
- 13 Solakidou, M., Theodorakopoulos, M., Deligiannakis, Y. and Louloudi, M., *International Journal of Hydrogen Energy*, **45**, 17367-17377.
- 14 Liu, H., Wang, W. H., Xiong, H., Nijamudheen, A., Ertem, M. Z., Wang, M. and Duan, L. *Inorganic Chemistry*, 2021, **60**, 3410-3417.
- 15 Ertem, M. Z., Himeda, Y., Fujita, E. and Muckerman, J. T., *ACS Catalysis*, 2016, **6**, 600-609.
- 16 Li, J., Li, J., Zhang, D. and Liu, C., *ACS Catalysis*, 2016, **6**, 4746-4754.
- 17 Britto, J. N., Rajpurohit, A. S., Jagan, K., Jaccob, M., *J. Phys. Chem. C*, 2019, **123**, 25061-25073.
- 18 Britto, J. N., Jaccob, M., *J. Phys. Chem. A*, 2021, **125**, 9478-9488.
- 19 Fellay, C., Yan, N., Dyson, P. J. and Laurency, G., *Chemistry -A European Journal*, 2009, **15**, 3752-3760.
- 20 Iguchi, M., Zhong, H., Himeda, Y. and Kawanami, H., *Chemistry -A European Journal*, 2017, **23**, 17017-17021.
- 21 Kawanami, H., Iguchi, M. and Himeda, Y., *Inorganic Chemistry*, 2020, **59**, 4191-4199.
- 22 Wang, T., Li, W., Chaoying, N., Anderson J., *Phys. Rev. Appl.*, 2018, **10**, 011003.
- 23 Huber, R., Spörlein, S., Moser, J.-E., Grätzel, M., Wachtveitl, J., *J. Phys. Chem. B*, 2000, **104**, 8995-9003.